Numerical Study of a Simplified Balanced Model

簡易平衡模式之數值研究

Chun-Tsung Wang

汪 群 從

摘 要

本文介紹一種四層簡易平衡模式供數值預報探討。所用模式範圍以侵台颱風爲主要探討對象，模式網格點距約 330 公里左右。模式設計供探討大幅度氣流運動，故初步僅考慮大幅度垂直氣流運動之熱機能。

經平衡方程式處理後之高度場，引用文中介紹之數值方法可模擬貝絲颱風侵台時之天氣變化現象。

1. Introduction

The application of numerical weather prediction and analysis techniques to the realm of tropical meteorology is currently demanding much effort and attention. Although at this time tropical weather data and data networks in the west Pacific are rather inadequate and inaccurate, series of studies have been underway to formulate limited area numerical weather prediction scheme for Taiwan area application. Along this line, barotropic, baroclinic as well as many other objective forecasting models are studied by the Atmospheric Physics Division of the Institute of Physics, Academia Sinica.

The present paper describes the development of a simplified four-level balanced model incorporating heat. Since feasibility study of using the model to simulate typhoon movement is the primary objective, only height data from weather map are used.

2. Model Design

The simplified governing equations for air movement, in the x, y, p, t coordintaes, are the vorticity equation, the balance equation, the energy equation and the equation of continuity (Haltiner, 1971)

$$\nabla^2\frac{\partial\psi}{\partial t}=-J(\psi,\eta)-\nabla\chi\cdot\nabla f+f\frac{\partial\omega}{\partial p} \quad \cdots\cdots (1)$$

$$\nabla^2\phi=f\nabla^2\psi+\nabla f\cdot\nabla\psi \quad \cdots\cdots (2)$$

$$\frac{\partial^2\phi}{\partial t\partial p}+J\left(\psi,\frac{\partial\phi}{\partial p}\right)+\nabla\chi\cdot\nabla\frac{\partial\phi}{\partial p}+\sigma\omega=-\frac{R}{pC_p}\cdot\frac{d(Q-\bar{Q})}{dt} \quad \cdots\cdots (3)$$

$$\nabla^2\chi=-\frac{\partial\omega}{\partial p} \quad \cdots\cdots (4)$$

where ψ is the stream function, ϕ is the geopotential height, χ is the velocity potential, ω is the vertical velocity, η is the absolute vorticity about the vertical, f is the Coriolis parameter, R is the specific gas constant, ($=287\ m^2/sec^2\text{-}K^\circ$), c_p is the specific heat capacity at constant pressure ($=1004\ m^2/sec^2-K^\circ$), Q is the heat energy, $\frac{d\bar{Q}}{dt}$ is the spatially constant radiational cooling (staff members, 1965), and $\sigma=-\frac{1}{\rho\theta}\frac{\partial\theta}{\partial p}$ is the static stability, where ρ is the air density, θ is the potential temperature.

The heating rate is approximated by

$$\frac{dQ}{dt}=\frac{dQ_S}{dt}+\frac{dQ_L}{dt} \quad \cdots\cdots (5)$$

where the sensible heating rate is (Gambo, 1963; Miller et. al. 1972)

$$\frac{dQ_S}{dt}=A\cdot|V_{1000}|(T_{sea}-T_{1000})\cdot\left(\frac{P}{P_{1000}}\right)^2$$

$A=0.001$ when $T_{sea}>T_{1000}$

$A=0.0001$ when $T_{sea}<T_{1000}$

$$|V_{1000}|\cong 0.7|V_{900}|=0.7\,(u_{900}^2+v_{900}^2)^{0.5} \quad \cdots(6)$$

$$u=\frac{\partial\chi}{\partial x}-\frac{\partial\psi}{\partial y}$$

$$v=\frac{\partial\chi}{\partial y}+\frac{\partial\psi}{\partial x}$$

and the latent heating rate caused by the ascent of moist air with the broad-scale vertical motion is (Danard, 1966)

$$\frac{dQ_L}{dt}=-LF^*\Delta S\ \omega \quad \text{when } \omega<0$$

$$=0 \quad \text{when } \omega\geqq 0 \text{ or } P\leqq 700\text{mb} \quad \cdots\cdots(7)$$

where u and v are velocity components in the x and y directions respectively, and u_{900} and v_{900} are that at 900mb, T_{sea} and T_{1000} are temperature at sea surface and 1000 mb level, V_{1000} and P_{1000} are velocity and pressure at 1000 mb level, v_{900} is velocity at 900 mb level. L is the heat of condensation ($=2.27\times10^6$ m^2/sec^2), and (Staff Members, 1973)

$$F^*=\left[\left(\frac{\partial q^*}{\partial p}\right)_T+\frac{RT}{c_p p}\left(\frac{q^*}{\partial T}\right)_p\right]\cdot\left[1+\frac{L}{c_p}\left(\frac{\partial q^*}{\partial T}\right)_p\right]^{-1} \quad \cdots\cdots (8)$$

$$q^*=0.622e[p-0.378e]^{-1}$$

$$T=-\frac{p}{R}\cdot\frac{\partial\phi}{\partial p}$$

$$e=6.11\left[\frac{273}{T}\right]^{5.31}EXP\left[25.22\left(1-\frac{273}{T}\right)\right]$$

$$\Delta S=1-\frac{T-T_d}{\Delta T'}\geqq 0 \quad \cdots\cdots(9)$$

where T_d is the dew point temperature, $\Delta T'$ is an empirical constant ($=5^\circ$K).

It is convenient to combine Eqs. 1, 2, 3, 4, 5, & 7 into the ωe-quation

$$\nabla^2\sigma^*\omega+f^2\frac{\partial^2\omega}{\partial p^2}=-\nabla^2\left[J\left(\psi,\frac{\partial\phi}{\partial p}\right)+\nabla\chi\cdot\Delta\frac{\partial\phi}{\partial p}+\frac{R}{c_p p}\cdot\frac{dQ_S}{dt}\right]+\frac{\partial}{\partial p}\left[-\frac{\partial}{\partial t}\nabla f\cdot\nabla\psi+fJ(\psi,\eta)+f\nabla\chi\cdot\nabla f\right] \quad \cdots\cdots(10)$$

where

$$\sigma^*=\sigma-\frac{R}{c_p p}\cdot LF^*\Delta S\geqq 0.2\sigma$$

$$\text{when } \omega<0 \text{ and } p>500\text{mb}$$

$$=\sigma \quad \text{when } \omega\geqq 0 \text{ or } p\leqq 500\text{mb} \quad \cdots\cdots(11)$$

3. Numerical Scheme

In solving Eqs. 1, 2, 4 & 10 for the four unknowns ψ ϕ χ and ω finite difference method is used. Difference grid systems are shown in Fig. 1. In the horizontal, a limited area computation domain is cut into $(NX-1)\times(NY-1)$ square meshes with mesh size $d\times d$. In the vertical, it is

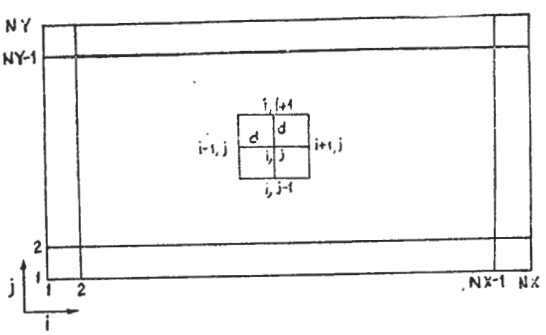

Horizontal grid system

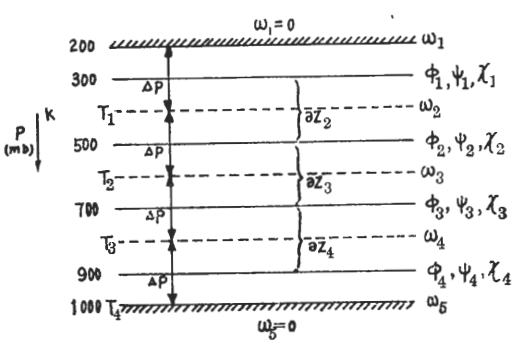

Vertical grid system

Fig. 1. Grid systems

tentatively cut into four even levels each 200mb apart. All unknowns are located at the grid points, where subscripts i, j, k are location index for their x, y and p direction positions respectively.

(1) *Data Initiation*

Geopotential height data, ϕ', at 200, 300, 500, 700 & 850mb are taken from weather map, height values at 900 mb level are evaluated from

$$\phi'_{900}=(32\ \phi'_{850}-14\phi'_{700}+3\phi'_{500})/21 \cdots\cdots (12)$$

Other weather data taken are sea surface temperature, Coriolis parameter, and mapping factor, m, at each grid points. $T-T_d$ values at 600 & 800 mb are arithmetically evaluated from weather data taken at 500, 700 & 850 mb. Then the following process is initiated to obtain the balanced weather data for numerical weather simulation.

a) Geopotential height data are filtered by using a 9 points smoothing operator (Shuman & Hovermale, 1968) to filter out high frequency components

$$\phi_{i,j}=\frac{1}{16}[4\phi'_{i,j}+2(\phi'_{i+1,j}+\phi'_{i-1,j}+\phi'_{i,j+1}+\phi'_{i,j-1})+(\phi'_{i+1,j+1}+\phi'_{i+1,j-1}+\phi'_{i-1,j+1}+\phi'_{i-1,j-1})] \cdots\cdots (13)$$

$[\nabla^2\phi+f^2]_{i,j,k}$ is then checked pointwise to make sure it is greater than zero in order to avoid imaginary solution in the balance equation. If $[\ ]_{i,j,k}$ is less than zero at certain grid point, it is set equal to zero at that point, and corresponding values at neighboring four points are each reduced by $0.25\ |[\ ]_{i,j,k}|$. Geopotential height field is thereafter relaxed to give the initial balanced geopotential height data.

In solving Laplace type equations, all difference equations are formulated by using center difference form, with the exception of Jacobian operator, J.

J is written as

$$J(A,B)=\frac{1}{3}(J^1+J^2+J^3) \cdots\cdots (14)$$

where

$$J^1=[(A_{i+1,j}-A_{i-1,j})(B_{i,j+1}-B_{i,j-1})-(A_{i,j+1}-A_{i,j-1})(B_{i+1,j}-B_{i-1,j})]/4d^2$$

$$J^2=[A_{i+1,j}(B_{i+1,j+1}-B_{i+1,j-1})-A_{i-1,j}(B_{i-1,j+1}-B_{i-1,j-1})-A_{i,j+1}(B_{i+1,j+1}-B_{i-1,j+1})+A_{i,j-1}(B_{i+1,j-1}-B_{i-1,j-1})]/Ad^2$$

$$J^3=[A_{i+1,j+1}(B_{i,j+1}-B_{i+1,j})-A_{i-1,j-1}(B_{i-1,j}-B_{i,j-1})+A_{i-1,j+1}(B_{i-1,j}-B_{i,j+1})-A_{i+1,j-1}(B_{i,j-1}-B_{i+1,j})]/4d^2 \cdots\cdots (15)$$

in order to preserve the square vorticity and kinetic energy (Arakawa, 1971). Laplace type equation, e. g. Eq. 2, could then be written in its difference form as

$$F(\phi_{i,j,k})=0 \cdots\cdots (16)$$

And a iteration procedure of

$$\phi^{n+1}_{i,j,k}=\phi^{n}_{i,j,k}-\frac{F(\phi_{i,j,k})}{\partial F/\partial\phi_{i,j,k}} \cdots\cdots (17)$$

is applied to solve the Laplace equation (Wang, 1971), where n and n+1 are two consecutive steps in the iteration process. New ϕ field values are used in Eq. 17 whenever they are available. Eq. 17 is repeatedly used until

$$\text{Max.}\ |\phi^{n+10}_{i,j,k}-\phi^{n}_{i,j,k}| \leq \epsilon\ (\phi) \cdots\cdots (18)$$

where ϵ is a pre-selected constant

$$\epsilon(\phi)=0.3$$
$$\epsilon(\omega)=10^{-6}$$
$$\epsilon(\chi)=100$$
$$\epsilon\left(\frac{\partial\psi}{\partial t}\right)=0.03 \cdots\cdots (19)$$

b). Balanced equation, Eq. 2, is solved to get the initial balanced stream function values, while on the boundary, stream function values are evaluated from

$$\frac{\partial\psi}{\partial s}=\frac{1}{f}\cdot\frac{\partial\phi}{\partial s}-\frac{\oint\frac{d\phi}{f}}{\oint ds} \cdots\cdots (20)$$

where s is the distance measured counterclockwise along the boundary and $\psi_{1,1}$ is arbitrarily set equal to $\phi_{1,1}/f_{1,1}$.

c). $\chi=0$ and $\frac{\partial\psi}{\partial t}=0$ are temporally assumed.

d). Solve ω-equation, Eq 10, to get ω field values.

e). Solve continuity equation, Eq. 4, to get χ field values.

f). Repeat d to e until the maximum difference between ω values at two consecutive cycles is less than 5×10^{-5} mb/sec.

g). Solve vorticity equation, Eq. 1, to get $\frac{\partial\psi}{\partial t}$ field values.

h). Repeat d, e, f, g, until the maximum difference between ω values at two consecutive cycles is less than 5×10^{-5} mb/sec The converging ω and χ field values are the initial balanced vertical velocity and velocity potential data for numerical computation.

(2) *Iteration Process*

a). For given ψ field values, solve Eq. 2, for ϕ field values.

b). Solve Eq. 10 for ω-field values,

c). Solve Eq. 4 for χ-field values.

d). Solve Eq. 1 for $\frac{\partial\psi}{\partial t}$ field values.

e). Repeat b to d until the maximum differences between ω values at two consecutive cycles are less than 5×10^{-5} mb/sec.

f). $\psi^{t+\Delta t}=\psi^{t}+\Delta t\cdot\frac{\partial\psi}{\partial t}$

at first time increment

$\psi^{t+\Delta t}=\psi^{t-\Delta t}+2\Delta t\cdot\frac{\partial\psi}{\partial t}$

at following time increments …… (21)

where Δt is the time increment. While satisfying von Neumann necessary condition (Staff Members, 1973), Δt is taken as 900 secs in the later case study.

Numerical computation proceeds by repeating a to f.

(3) *Boundary Conditions.*

The following boundry conditions are used for the present balanced model study.

a). In the vertical direction, vertical velocity is assumed to be zero at 200 and 1000 mb levels.

b). At the lateral boundary, vertical velocity, velocity potential, $\frac{\partial\psi}{\partial t}$ and $\frac{\partial\phi}{\partial t}$ are assumed to be zero.

c). When ψ and χ values outside the computation domain are needed, free-slip boundary condition (Welch et. al., 1965) assumption gives ψ value one layer outside the boundary to be equal to two times ψ value at the boundary deduced by ψ value one layer inside the boundary, while χ value outside the boundary to be equal to its image value inside the boundary.

d). When ϕ values outside the computation domain are needed for computation, geostrophic wind assumption at the boundary gives ϕ value one layer outside the boundary to be equal to two times ϕ value at the boundary deduced by ϕ value one layer inside the boundary.

4. Case Study

Numerical study of the four-level balanced model is made on Typhoon Bess of September 21, 1971. A grid system ($d=3\,322\times10^{5}$m, NX=20, NY=14) is set to cover an area approximately 6,650km ×

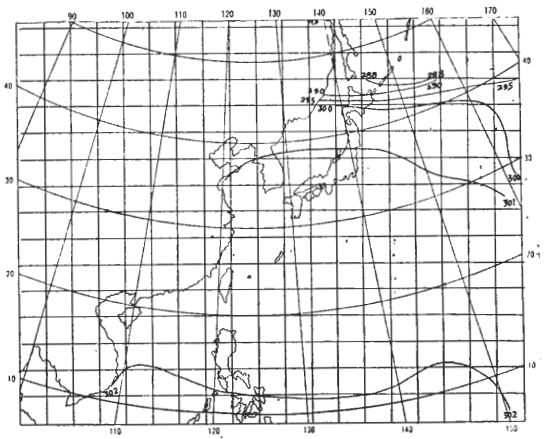

Figure 2. Computation domain & T_{sea} field (°K)

4,650km, with the Island of Taiwan located around [i=9, j=6]. This computational domain is arbitrarily chosen and should not be regarded as the best selected limited area domain for Typhoon Bess study.

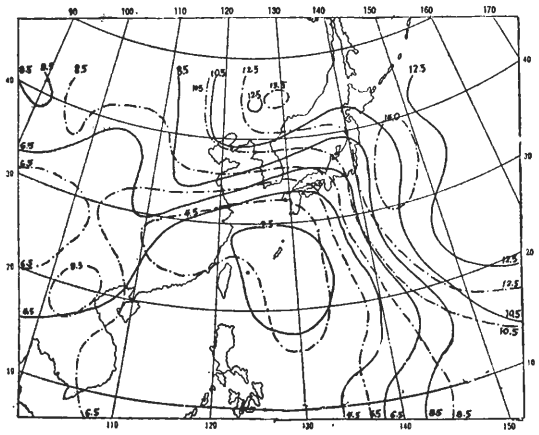

Figure 3. $T-T_d$ data

—— · —— p=600mb

———— p=800mb

Figures 2 & 3 show the surface temperature and $T-T_d$ fields, they are assumed to remain unchanged throughout the computational time domain for computational

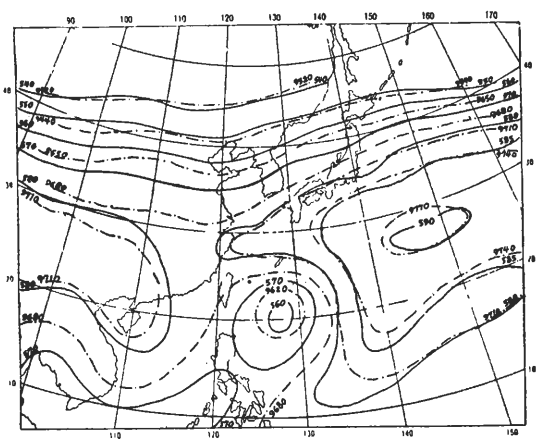

Figure 4. Stream function & geopotential height data

time=0 hr.

p=300 mb

—— · —— ϕ/g (m)

———— ψ ($\times 10^6$ m^2/sec)

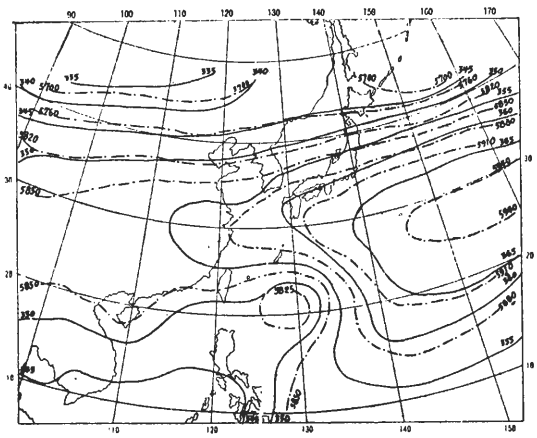

Figure 4. Stream function & geopotential height data

time=0 hr.

p=500 mb

—— · —— ϕ/g (m)

———— ψ ($\times 10^6$ m^2/sec)

sake, Figure 2 shows that near typhoon track, sea surface temperature is around 302°K, while Fig. 3 shows that the $T-T_d$ field after its short wavelength components being filterd out by using a five points smoothing operator (Staff Members, 1973). It is clear that $T-T_d$ gets smaller when air is close to the sea surface or to the typhoon center.

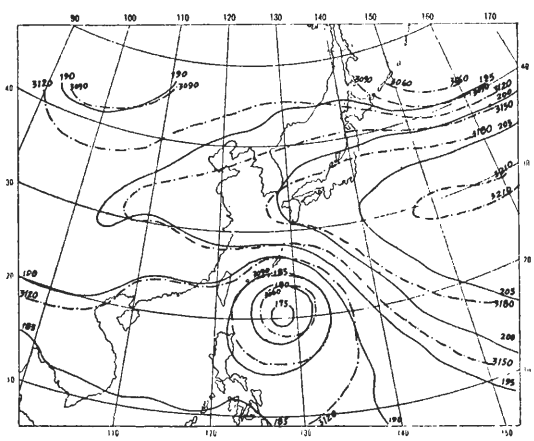

Figure 4. Stream function & geopotential height data

time=0 hr.

p=700 mb

—— · —— ϕ/g (m)

———— ψ ($\times 10^6$ m^2/sec)

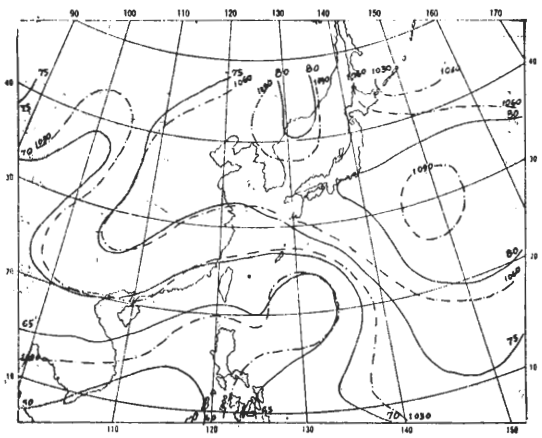

Figure 4. Stream function & geopotential height data
time=0 hr.
p=900 mb
—·— ϕ/g (m)
——— ψ ($\times 10^6$ m²/sec)

Figure 4 shows the initial balanced geopotential height and stream function fields after data initiation, with typhoon centered around [i=12, j=6], i. e. N23°, E 130°, at 900mb level and skewed toward left [i=11, j=5] at 300mb level. It should be mentioned that typhoon center pressure has been increased from the initial weather map reading of 964m to the smoothed data reading of 982m after the data initiation process. Wind blows in the counterclockwise direction around typhoon center, being maximum in the north-east corner of the typhoon. Vetical velocity is negative in front of the center and is positive behind the center, lined in the north-west direction. (Short of CalComp Plotter, these are not shown).

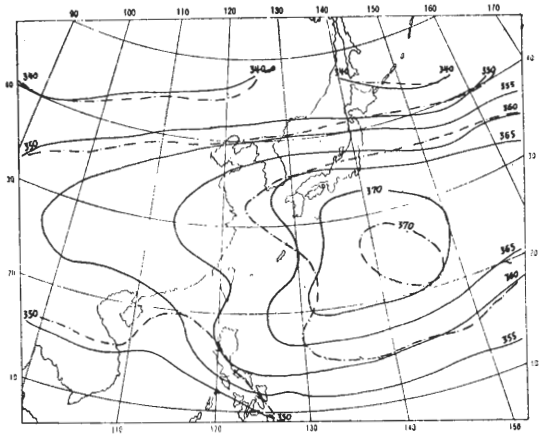

Figure 5. Stream function data ($\psi \times 10^6$ m²/sec)
p=500 mb
—·— time=12 hr.
——— time=24 hr.

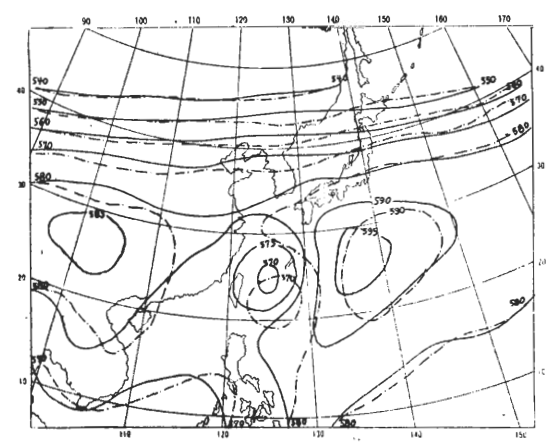

Figure 5. Sream function data ($\psi \times 10^6$ m²/sec)
p=300 mb
—·— time=12 hr.
——— time=24 hr.

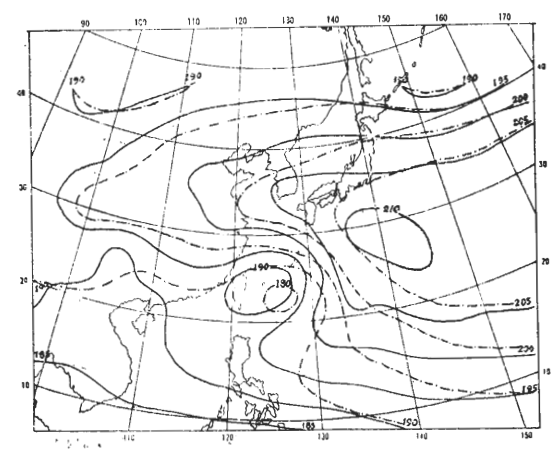

Figure 5. Stream function data ($\psi \times 10^6$ m²/sec)
p=700 mb
—·— time=12 hr.
——— time=24 hr.

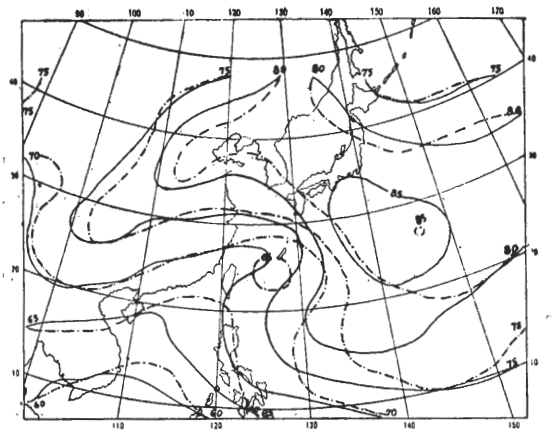

Figure 5. Stream function data
($\psi \times 10^6$ m²/sec)
p=900 mb
—·— time=12 hr.
——— time=24 hr.

Figure 5 shows the stream function fields after 12 and 24 hrs. It is seen that the typhoon center moves approximately in the north-west direction. After 24 hrs, typhoon centers around N 25°, E 124° at 900 mb level, arouad N 24.5°. E 124° at 700mb level, and around N 25°, E 125° at 300 mb level. The high pressure field in the east part of the computational domain also moves west. This is similar to the real typhoon track.

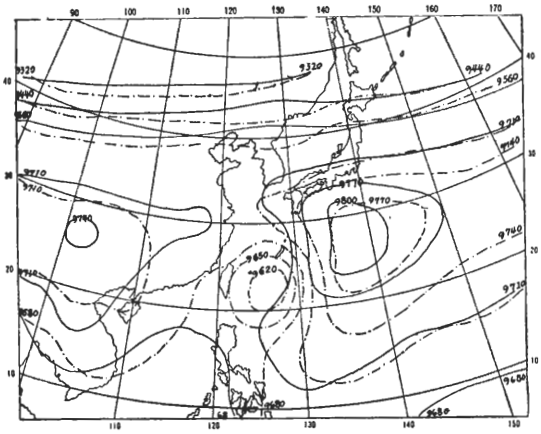

Figure 6. Geopotential height data
(ϕ/gm)
p=300 mb
—·— time=12 hr.
——— time=24 hr.

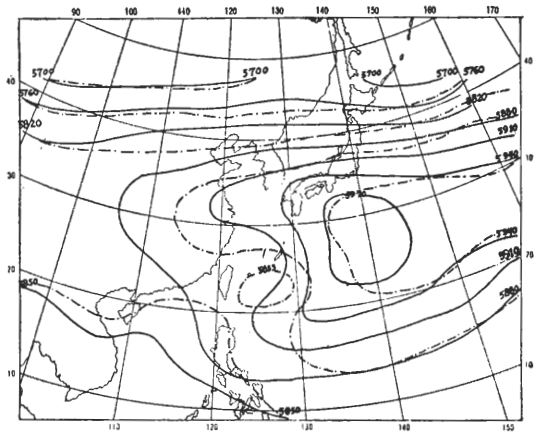

Figure 6. Geopotential height data
(ϕ/g m)
p=500 mb
—·— time=12 hr.
——— time=24 hr.

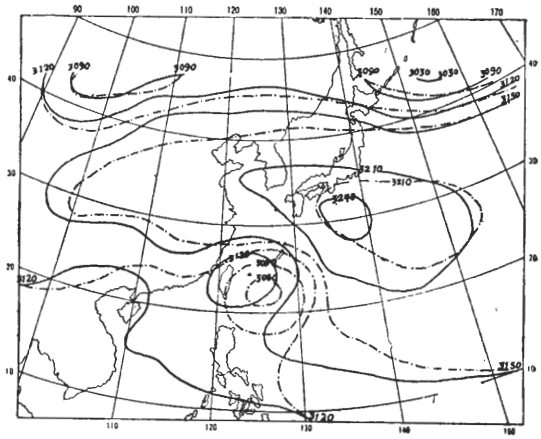

Figure 6. Geopotential height data
(ϕ/g m)
p=700 mb
—·— time=12 hr.
——— time=24 hr.

Figure 6 shows the geopotentential height fields after 12 and 24 hrs. The change in weather pattern is quite similar to that of the stream function field, it is also similar to that obtained by using a four-level baroclinic model (Staff Members, 1973) except that the field filled much faster possibly due to the initial smoothing process.

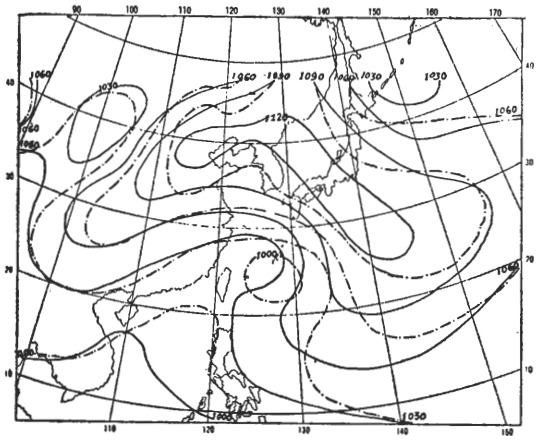

Figure 6: Geopotential height data (ϕ/g m)
p=900 mb
—·— time=12 hr.
——— time=24 hr.

Test run with another simplified heating function

$$\frac{LF^*}{C_p}=0.06$$

$$\Delta T'=7.5$$

is also made, which gives results nearly identical to that given above.

5. Summary

Numerical study on Typhoon Bess of September 21, 1971 by using a simplified four-level balanced model incorporating heat is made. Stream function and geopotential height are related through the balance equation, their initial balanced data are manipulated from weather map contours. The model with grid mesh size of about 330 km is designed primarily for synoptic-scale studies, thus only broad-scale vertical air motion is considered in the heating function. With the numerical scheme designed, the model successfully simulate the movement of Typhoon Bess.

Acknowledgments: The author is grateful to Miss, C. I. Shiau for her many helps in making this study possible. Thanks are also to the National Council for its financial support.

References

Arakawa, A., Design of the UCLA General Circulation Model, Dept. Met., UCLA, 1971

Danard, M. B., A Quasi-geostrophic Numerical Model Incorporating Effects of Latent Heat, J. Appl. Met., 5, 85, 1966.

Gambo, K., The Role of Sensible and Latent Heats in the Baroclinic Atmosphere, J. Meteo. Soc. Japan, 41, 233, 1963.

Haltiner, G. J., Numerical Weather Prediction, John Wiley & Sons, Inc., N. Y., 1971.

Miller, B I. et. al., Numerical Prediction of Tropical Weathering Systems, MWR, 100, 825, 1972.

Staff Members of Electronic Computation Center, 72-hr. Baroclinic Forecast by the Diabatic Quasi-Geostrophic Model, J. Meteoro. Soc. Japan, 43, 246, 1965.

Staff Members of Atmospheric Division, Simulation Model for Atmospheric Motion: III: Heat and Friction, Ann. Rept., Inst. Phys., Academia Sinica, 1973.

Shuman, F. G. & J. B. Hovermale, An Operational 6-layer Primitive Equation Model, J. Appl. Met., 7, 525, 1968.

Wang, C. T., Drop-Water Impact, Ann. Rept. Inst. Phys., Academia Sinica, 107, 1971.

Welch, J. E. et al., The MAC Method, LA3425, U. Calif. Los Alamos, 1965.

作者通信處：南港中央研究院物理研究所